NASA Technical Memorandum 81702

Diagnostic System Design for the Ion Auxiliary Propulsion System (IAPS)—Flight Test of Two 8 cm Mercury Ion

E. B. Hurst
Lewis Research Center
Cleveland, Ohio

and

G. Z. Thomas
Hughes Aircraft Co.
Los Angeles, California

Prepared for the
Fifteenth International Electric Propulsion Conference
cosponsored by the American Institute of Aeronautics and Astronautics,
the Japan Society for Aeronautical and Space Sciences,
and Deutsche Gesselschaft fur Luft- und Raumfahrt
Las Vegas, Nevada, April 21-23, 1981

NASA

DIAGNOSTIC SYSTEM DESIGN FOR THE ION AUXILIARY PROPULSION SYSTEM (IAPS) - FLIGHT TEST OF TWO 8 cm MERCURY ION THRUSTERS

E. B. Hurst*
NASA Lewis Research Center
Cleveland, Ohio

and

G. Z. Thomas**
Hughes Aircraft Co.
Los Angeles, California

Abstract

The Diagnostic Subsystem (DSS) is a part of an Ion Auxiliary Propulsion System (IAPS) that is scheduled to be flown on P80-1 spacecraft in May 1983. The report explains the mechanical, thermal, electrical design and the ground test results of four types of detectors. The DSS is designed to measure the thruster efflux material deposition and S/C potential relative to the local plasma in the vicinity of two 8 cm mercury ion thrusters. The DSS consists of two quartz crystal microbalance (QCM) detectors, one potential probe, nine solar cell arrays, seven ion collectors and two electronic packages.

Introduction

The P80-1 spacecraft (S/C) is being developed by Rockwell International (RI) for the Air Force. The S/C will be launched in the Shuttle to a parking orbit of 296 kilometers (km) and then transferred to a final orbit of 740 km by two solid rocket motors (TE-M-364-4) developed by Thiokl Chemical Corporation. The S/C is designed to carry four experiments (Fig. 1) into an orbit with a minimum inclination of 72.5°. The principal experiment, Teal Ruby, is developed by RI for the Defense Department. The second experiment is an Ion Auxiliary Propulsion System (IAPS) developed by Hughes Aircraft Company for NASA-Lewis Research Center. The third experiment is an Extreme Ultraviolet (EUV) imaging telescope developed by the University of California at Berkley. The fourth experiment is a Lasercom Space Measurement Unit (LSMU) developed by McDonald Douglas Astronautics Company for the Air Force. The IAPS mission represents the culmination of the technology verification of the 8 cm mercury ion thruster system and the associated power, control and propellant components necessary to configure an ion propulsion system for satellite control. The hardware consist of two 8-cm mercury ion propulsion subsystems and one Diagnostic Subsystem (DSS). The purpose of the IAPS is to flight qualify the system for possible use in station keeping, attitude control and orbit maneuvering for future S/C. Each of the ion auxiliary propulsion subsystem are located in separate modules (Figs. 2 to 4).

The DSS is composed of several detectors to detect and measure thruster efflux, material deposition and S/C potential relative to the local space plasma. The DSS detectors are clustered around each of the thrusters. Most of the detectors are located behind or in line with the edge of the beam shield located on the thrusters. A special ground plane (less than 1000 ohms per square) is located on the module surface between the detectors (Fig. 5).

These DSS detectors are to be activated soon after launch in order to establish a reference data base before the ion thrusters are operated. The DSS detectors are operated and controlled by two electronic units that are located inside the zenith module. The DSS detectors consist of two QCM units, nine solar cells arrays, seven ion collectors and one potential probe.

This report explains the mechanical, thermal, and electrical design and presents the ground test results obtained for the four types of detectors.

Overview of the DSS

The DSS is designed to quantify the thruster efflux, material deposition and S/C potential in the vicinity of two ion mercury thrusters. The QCM's measure frequency in the range of 2 to 65 K Hz. The solar cell arrays have the capability to measure current and voltage from 0-600 mA and 0-0.9 V. The ion collectors are capable of measuring ion current from 10^{-3} to 10^{-9} amperes with bias voltages of 0, 25, 55 and 96 V. The potential probe can measure current at 16 different commandible levels varying from one (1) to 5 K microamperes within a voltage range of -25 to 175 V.

The DSS weighs 27 kilograms and requires 27 watts of power to operate in space. The DSS is qualified for space flight.

QCM Package

The QCM Package consist of two temperature controlled detectors and an electronics unit. The No. 1 QCM detector is located directly in back of the thruster beam shield on the zenith surface 40 centimeters above the thruster grid plane (Fig. 2). The second detector is located on the -x surface of the S/C in line with the edge of the thruster beam shield 17.5 centimeters below the grid plane. The detector detailed design and configuration are proprietary with Berkeley Industries, 2825 Laguina Canyon, Laguna, California. The conceptual arrangement is illustrated in Figs. 6 and 7. The detector assembly (7 by 5 cm) weighs 350 grams (Fig. 8).

Theory and Purpose

The quartz crystal microbalance detector is used for measuring the mass of material that may deposit on the exposed surface. The crystal oscil-

*Aerospace Engineer.
**Section Head.

lates in a horizontal direction (thickness shear mode). Mass deposited on the surfaces decreases the resonant frequency of the exposed crystal. Two crystals are located in the detector head. One crystal is exposed to the environment and the other crystal is unexposed and acts as a reference. The resonant frequency of both crystals are excited by dual oscillators located in the detector housing. The resultant frequency is obtained as the difference, or "beat", frequency. As the mass is increased on the exposed crystal the beat frequency is increased. For converting beat frequency to mass the standard sensitivity equation for this type of crystal will be used (ΔM = Area x 4.43×10^{-9} grams/cm^2 Hz). The temperature of the crystals are controlled to 25°±1° C. This is done to minimize any temperature-induced frequency shifts and to maintain an isothermal surface for contamination purposes.

Detector Crystal

Both crystals are identical in shape and size. Each crystal (1.24 cm diam) has a resonant frequency of 10 MHz (Fig. 9). Each crystal is optically polished before vacuum deposited aluminum (6000 Å thick) is applied to the front and back of the surface (Fig. 10). The effective area of the crystal is 0.810 cm^2. The exposed surface is covered with Magnesium Floride (1600 Å). Two teflon constantan wires are attached to the crystals with silver filled epoxy (Dupont 5504A) 180° apart. These wires are coiled to reduce excessive stresses due to handling and qualification testing. In addition, the coiling provides a long thermal path to improve the peltier cooling efficiency. The two crystals are held in assembly by four low-load springs.

Temperature Sensor

A platinum resistance thermocouple (PRT) is located between the active and reference crystal. The PRT is shielded from the active crystal with an aluminum plate. The PRT mounting plate shields the reference crystal. The PRT is epoxied to the mounting plate with stycast 2850FT and catalyst 24LX (Emmerson Cummings).

Heat Pump

The thermoelectric heat pump controls the temperature of the crystals at 25°±0.68° C. The semiconductor unit is supplied by Marlo Industries. The heat pump is cemented directly to the heat sink and the mounting plate. In the cooling mode heat is dissipated to the heat sink, when dc current flows from the N-type to the P-type semiconductor. In the heating mode heat is absorbed from the heat sink, when the dc current flows in the opposite direction. The cooling and heating rates are approximately 0.5° per second (Fig. 11).

Heat Sink and Mounting Flange

The flange was designed to provide the thermal requirements for controlling the temperature of the QCM crystals and to be compatible with the heat pump size.

Cover

The cover is fabricated of aluminum with a polished surface. The surface parallel with the crystal is covered with electroless nickel to lower the radiation to the head.

Electronics

Dual oscillator/mixer hybrid chip elements are located in the back portion of the detector assembly. These oscillators drive the crystals at their natural frequency. The electronics unit receives the 28±6 volt power and converts it to signal and thermal control power. The frequency signal is converted into a 16 bit compatible parallel digital output word to the DSSCU (Fig. 12). The unit also provides the timing signal for the frequency count, receives and controls the temperature signal for the thermoelectric cooler and develops a 5.12 volt analogue signal for defining crystal temperature. The electronics unit (19 cm long by 15 cm high by 15 cm wide) weighs 2.74 kilograms (Fig. 13). The electronics unit is qualified for flight on P80-1.

Test Results

On the basis of the test data taken in the laboratory QCM Nos. 1 and 4 were selected for flight. Initially both of these detectors were tested in vacuum without using the thermal controls. This gave a baseline for comparison purposes. Without temperature control the frequency varied as much as 125 Hz over a temperature range of -20° to +50° C (Fig. 14). With the thermal control operating as designed, the temperature of the crystals was maintained within 25°±1° C. The frequency output in this case varied only 26 Hz (Fig. 15). Solar Irradiance induced transients data indicated in the laboratory that frequency can shift as much as 70 Hz (Figs. 16 and 17). Adding the frequency shifts due to the temperature variable and the solar irradiance, the expected accuracy can vary as much as 91 Hz (Table 1). However, these frequency shifts are predictable and can be accounted for in data reduction with this known data and in flight calibrations. The power required to operate the two detectors and electronics varies from 1.5 to 5.5 watts depending upon the temperature in flight (Fig. 18). The thermoelectric cooler is slightly more efficient when the environment is warm.

Solar Cell Detectors

Nine solar cell arrays (each 13.64 cm^2) detect the deposition of materials by measuring the degradation of the current output across a one ohm resistor. The deterioration of the radiator cooling performance also gives a measure of the deposition of a larger adjacent surface by measuring the temperature shift before and after contamination. The nine solar cell arrays and four radiator surfaces are located around the thruster (Fig. 2). The solar cell surface is at an angle of 45° with the thruster grid plane and 45° to the S/C orthogonal axes. All deck mounted solar arrays have the same view factor to the sun. Five arrays are located on the X-module. One array (C_3) is located directly in back of the beam shield and 50 centimeters above the thruster grid plane. The surface of this array is perpendicular to the thruster grid plane. The other eight solar cell arrays are located in pairs of two, one a warm array and the other cold.

The four warm arrays are mounted on aluminum brackets (Figs. 19 and 20) that are fastened directly to the Module surface. This arrangement provides a thermal path to the inside of the Module. The four cold arrays are mounted on large heat sinks. Radiator surfaces are mounted on these same heat sinks to keep them cold. The radiator, solar array,

and heat sink assembly is mounted to a fiberglass bracket to thermally isolate it from the Module. Thermal blankets are wrapped around the fiberglass bracket to further isolate the cold array from the deck and its companion warm array.

Radiators

The surface of the radiator consists of ten thermal control mirrors (Fig. 21). Each cover glass (0.015 cm thick by 2.33 cm wide by 6.48 cm long) has an anti-reflective and ultraviolet radiation protective coating of silver with overcoat layers of inconel and indium oxide. The mirrors are bonded to a 0.95 centimeter thick aluminum plate with RTV-566 mixed with 10 percent carbon. The interstices are covered with reflective paint. In the flight configuration the fiberglass bracket is covered with ten layers of kapton covered super insulation. These radiators are designed to limit the orbital variation of temperature to 8° C. An extra weight of 0.45 kg is attached beneath each radiator to maintain this temperature variation limit per orbit. The radiator is parallel to the thruster's grid plane. The warm and cold solar cell arrays are in the same plane and are located twelve centimeters upstream of the accelerator grid plane and 60 cm radius from the thruster centerline.

Thermal Design

The design of the solar cell array and radiator was governed by the temperature requirements. One of the design goals was to obtain passively -80° C for a period of 500 continuous hours during the flight. This low temperature would assure condensation of mercury on the cold surfaces. Since the solar cell arrays and radiator mounting had to be designed early, little thermal data was available from the S/C contractor. Therefore assumptions were made as to the S/C temperature and the orbit parameters. Based on the assumption listed in Table 2, orbital average temperatures were predicted for various right ascertion angles at the vernal Equinox season. The effect on temperature performance due to various surface areas, weight, S/C mounting location, thermal degradation and thermal interchange with other IAPS components were determined. Orbital heating data was generated for right ascertion angles of 60°, 180°, 240°, 270°, 300° and 360°. The data for the right ascertion angle of 270° (Fig. 22) is representative for this paper. The initial study used the Z-module as a baseline with no albedo earth loads. This thermal study indicates that the cold solar array surface radiator will be in the range of -50° C (Figs. 23 and 24). The design goal of -80° C for 500 hours is not achieveable with passive design. The temperature of the radiator and cold solar cell array will vary with each other less than 2° C during orbit. The variation in average normal illumination between the radiator and solar array surfaces is shown in Fig. 25. The average illumination of the radiator is 8.8 percent while the average illumination on the solar cell is 37.2 percent.

Electronics

The solar cell electronics is located in the DSSCU. Each of nine solar cell arrays is shunted by a precision one ohm wire wound resistor which produces a voltage proportional to the cell current (Fig. 26). The voltage is amplified by the first stage amplifier. The second stage amplifier with the input from the analog comparator sets the dual slope starting point at 20 percent of the solar radiation level.

Temperature Sensor

The temperature sensor elements are wired into the feedback network of an operational amplifier (Fig. 27). Since the gain of the operational amplifier depends on the ratio of the feedback resistor to the summing resistor, as the resistance of the temperature sensor changes with temperature, so also the gain of the operational amplifier changes proportionally. By applying a fixed reference voltage to the input of the operational amplifier the exact output of the operational amplifier can be determined by knowing the resistance of the temperature sensor. Conversely calculating backwards from the output voltage of the operational amplifier and determining the resistance of the temperature sensor the temperature of the sensor can be extracted from the calibration data.

However, since the temperatures of the hot and cold cells may differ from each other by a wide margin, to keep the outputs of the operational amplifiers within the measurement range of the analog to digital converter, the operational amplifier is followed by a scaler operational amplifier which maintains the voltage within 0 to +5V limits. The resistor elements used for the operational amplifiers are all 1 percent tolerance to reduce error. They are all metal film to reduce their variation with temperature.

Temperature Ranges

The cold solar cell temperature measurement ranges from +25.5° to 102.5° C (Fig. 28). The warm solar cell temperature measurement ranges from -27.5° to 100.5° C. The proportional constant equal 0.040 volts per degree centrigrade. During the thermal vacuum test on the hot side (+80° C) the variation was less than ±1° C. The temperature sensors are calibrated to an accuracy of less than 0.1° C. All thirteen sensors deviated less than ±0.25° C from the calibration curve. The conversion from resistance to voltage in the temperature electronics follows a straight line with an error of less than 0.5 MV (0.01° C). The telemetry output data accuracy is better than 2° C.

Solar Cell Calibration Curves

The interpretation of the voltage and current data from the solar cell arrays is more difficult (Fig. 29). The current output is affected by the sun angle, temperature at the surface and the degradation due to the radiation level. The current output based on laboratory tests indicates that the output can vary as much as ±10 percent based on temperature and radiation variation. Assuming that the sun angle and temperatures of each array are known, the only other variable is the radiation. Assuming a radiation level of 1×10^{14} electrons per cm^2, the current output can drop as much as 9 percent at -100° C. However, the radiation is based on a long term effect. By keeping a good record of the reference data base, small changes in current output can be ascertained.

Ion Collector Detectors

The ion collector (IC) detectors consist of seven units located around the thrusters (Fig. 2).

Four units are located on the zenith module and the other three are located on the X-module. Six units are placed 15 cm below the thruster grid plane and the seventh is located 10 cm above the grid plane. Six units are 60 cm away from the thruster and the seventh is 20 cm away. The preamplifier for the electronics is located in the ion collector housing to lower the noise level. This also raises the voltage level to 0-5 volts range for transmission to the DSSCU. Each unit is 13.95 cm diam by 5.21 cm deep and weighs 0.66 kilograms (Figs. 30 and 31). The collector plate and the grids are isolated from the housing with fiberglass spacers and separators (10^{12} ohms).

Theory and Purpose

The IC detectors measure the low level ions that are upstream of the mercury ion thrusters. The IC's are also sensitive to the ambient environmental fluxes. The grid potentials are selected to keep out electrons and also to reflect secondary electrons from the collecting plate. The biasing grid voltage is basically a retarding potential with four commandable constant voltage levels. The collector plate auto-ranges to six different separate current levels when the density of the ions require it.

Mechanical Alignment

The six mounting holes in each set of four grids were drilled simultaneously using a fixture. This method of manufacturing permitted aligning the openings in all four within 0.01 cm of each other.

Grids

The grids were electron discharge machined (EDM) from 0.0.22 cm thick non-magnetic (301) stainless steel. The openings in the grids exceed 72 percent of the exposed area. These openings are 0.16 cm square over a diameter of 8.66 cm diam (Fig. 32). The ground screen grid (ground potential) and biasing grid (0, 25, 55, 96 V) have an exposed area of 8.05 cm diam. The shielding grid (-12 V) and supression grid (-12 V) have an exposed area of 8.64 cm diam. The grids are spaced 0.30 cm apart (Fig. 33).

Separators and Isolators

The separators and isolators consist of epoxy glass that provide isolation of 10^{12} ohms of resistance. The separators also provide the proper grid openings and shadow shielding of the cylindrical mounting isolators.

Collector Plate

The collector plate (7.50 cm diam by 0.16 cm thick) was machined from 6061-T6 aluminum plate. The collector side is covered with 2000 Å of sputtered molybdenum. The collector plate is mounted to a fiberglass base by three threaded extensions on the back of the plate. The base (11.50 cm diam by 0.86 cm thick) is fastened to both the housing and cover of the IC.

Preamplifier/Scaler

The preamplifier/scaler electronics are mounted on a circular printed wiring board that is sandwiched between the cover and the base. A block diagram of the electronics is shown in Fig. 34. The scale factor used for this circuit depends upon the logic input signal from the autorange logic board in the Diagnostic Subsystem Control Unit (DSSCU) which selects the proper current range from 10^{-3} to 10^{-8} amperes.

Thermal Design

A thermal analysis was performed on the ion collector in order to predict the temperature behavior of the circuit board in back of the ion collector. Based on the solar cell detector thermal analysis, a 37 percent normal illumination incident was assumed. Accounting for the screen grid shadowing, the collector plate intercepts 35 percent of the incident radiation. With a module deck temperature of -20° to +50° C, the ion collector circuit board will experience -31° to +65° C. This assumes that all exterior surfaces, except the screen area, are covered with thermal blankets (10 layers of 1/4 mil crinkled aluminized kapton and an inner and outer layer of 1 mil aluminized kapton, kapton side out).

Electrical Design

A simple block diagram of the electronic system design is illustrated in Fig. 35 for one of seven ion collectors.

Test Results

The measured resistance between the collector plate and detector housing, the shielding grid, biasing grid and detector housing are in the 10^{12} ohms resistance range. The current range on the collector plate has the full range of 10^{-9} to 10^{-3} amperes in decade steps. At the lower binary count in the 10^{-8} amperes range the maximum variation was four bits (4 out of 256). The ammeter autoranges up or down in a maximum time of 0.9 seconds per range and settles out within ±2 percent of the final value within 1 second. The telemetry output for the current is linear over each of the six ranges (±3 percent over the full range). The shielding and supression grids are shielded at -12±1 volts. The biasing grid receives on command the following voltages: 0±0.5 volt, 25±2 volts, 55±2 volts and 96±2 volts. The load line for each of the bias voltages is linear and parallel within 2 percent.

Potential Probe Detector

The probe (0.83 kg) consist of a hollow sphere (24.23 cm diam) attached to a post (3.5 cm diam by 38 cm long) with double shadow shields (Figs. 36 and 37) attached near the base. The probe is located on the Z-module 60 cm away from the thruster. The spherical surface is located 25 cm away from any conducting surface.

Theory and Purpose

The potential probe is basically a Langmuir probe. It is essentially a precision current source driving a spherical electrode external to the spacecraft. Current is commanded to the unit in sixteen different current levels varying from 1 to 5000 microamperes. The voltage developed must range from -25 to -175 volts simulating plasma conditions.

Sphere

Two hemispheres were hydro-formed from 0.05 cm thick aluminum sheet (6061-0). These two hemispheres were welded to a center aluminum plate (0.23 cm thick) that serves as a center mounting for attaching the post. The outside of the sphere was coated with 2000 Å of gold.

Post

The post is isolated from the module (10^{12} ohms) by use of fiberglass materials. The post is fastened to the center plate by using a long wrench that extends from the bottom of the post. The base and post were increased in size due to failures during vibration of the verification model. Fiberglass shadow shields are bonded to the post near the base to avoid possible coating on the post during space operation. The three wires are bonded to the center plate before the welding of the plate and hemispheres and then pulled through the post before the post is fastened to the center plate. Two wires are used for redundancy.

Electronics

A functional block diagram of the circuit is shown in Fig. 38. The system is a basic servo-loop with a constant reference voltage as input. The input to the integrator is nulled when the voltage across the selectable resistance is 10 volts. Because the unity-gain buffer draws very little current, virtually all current passing through the resistor is conducted to the sphere with the voltage across this resistance held constant, current to the sphere is constant and thus depends upon the valve of the resistance. This is true provided that the necessary voltage can be attained by the high voltage amplifier.

Test Results

The potential probe package is a highly reliable and accurate system that has been qualified for flight. The potential probe has passed 20 GRMS random vibration in three axes. The electronics has survived two thermal vacuum cycles at -30° to +60° C operating and one cycle at -50° to +80° C nonoperating. The electronics also withstood nine thermal cycles at the extreme temperatures. The accuracy of the telemetry current reading is within ±2 percent of full scale for each of the following 16 ranges in microamperes: 1.00, 1.76, 3.11, 5.49, 9.69, 17.1, 30.2, 53.3, 93.9, 166, 292, 576, 910, 1610, 2830 and 5000. The accuracy of the telemetry voltage is ±1 volt from 0-50 volts and ±2 volts from 50 to 125 volts.

Diagnostic Subsystem Control Unit (DSSCU)

Due to the many common functions such as power distribution, data formating, commands and telemetry the DSSCU was designed to contain the electronics for seven ion collectors, nine solar cells and one potential probe into one subassembly (Fig. 39). Twenty electronics boards and one dc-to-dc converter are located in this unit (Figs. 40 and 41). The package (44.45 cm long by 21.6 cm wide by 16.20 cm high) weighs 28.97 kilograms and requires 22 watts of power to operate all detectors. The electronic boards are located in five separate compartments to permit dissipation of heat and to provide structural rigidity. The package has the capability of turning off and on any one type of detector. Two separate multiplexers are included to provide redundancy. This package is located in the Z module and controls the detectors in both the Z and X modules. All nine cable connectors are located in the top portion of the assembly. The electronic boards are installed from the side of the package. The front panel provides a means of preloading the electronic boards. Flexible material is installed on the inside of the front panel. The joining of the panels also permits minimizing EMI/EMC leaks. This is accomplished by avoiding straight line paths to the inside of the package. The dc to dc converter is isolated from the electronic boards. The metal thicknesses chosen on the DSSCU, plus the module honeycomb surface (1.2 cm thick) of the module, provides adequate shielding (7000 rads for a three year period).

Commands and Data

The S/C has the capability of switching the power OFF or ON to the DSSCU and selecting either mux A or B. The DSSCU is designed to accept a number of discrete commands from the spacecraft. These allow each of the four detector groups to be commanded ON or OFF. Also the DSSCU is designed to accept 16 bit serial magnitude commands from the S/C for controlling the IC and potential probe. Actually only bits 8 and 9 (Ion collector) and bits 10-13 (potential probe) are used. The minimum time between command transfersis is 16 seconds. The last command to the DSSCU is telemetered back to the S/C.

The DSSCU has two identical serial data circuit outputs on separate lines to the S/C. Each circuit consists of four lines which provide a data enable envelope, a clock signal and a data line. The S/C allocates eighty bits of DSSCU data output in each one second frame. The DSSCU furnishes this to the S/C as one 8 bit word per 0.1 second continuously. The DSSCU provides a new 8 bit serial digital output each 0.2 seconds to the telemetry. All data is provided in a specified sequence (Table 4) which is synchronized with the S/C telemetry system by the use of a frame sync signal. Bilevel measurements are also provided by the DSSCU to indicate which mux was selected.

Housing

The main structure was machined from a single aluminum bar (7075-T651). The thickness of the base (0.48 cm nominal) was varied to provide for mounting of components and for dissipation of heat to the module. Openings in the sides and top (0.24 cm thick) of the structure were provided for access and installation of electronic boards. Separate front and back panels (0.24 cm thick) were fabricated for closing the openings. The top panel was added to provide for all connections (9) and cabling.

Electrical Design

The DSSCU was designed to conform to the Interface Control Document (ICD) with the spacecraft contractor. The power required to operate the DSS was also limited. The original design concept was based on using commercial available components and electrical parts. This concept proved more difficult than imagined. Electrical components were not available to provide the efficiencies desired. Even commercial electrical parts had long procurement cycles.

dc to dc Converter

meet the limited power available it was decided to have an efficient power source that can receive 22-34 volts from the spacecraft bus and can convert this voltage to a variety of detector circuit requirements. The dc to dc converter is required to meet the voltage and current requirements of the ICD and supply five dc voltages varying from 210 to -40 V dc (Fig. 42). Originally a commerical dc to dc converter was selected to provide controlled voltages to the various detector circuits. After testing this unit with the DSS verification model, the dc to dc converter proved to be only about 38 percent efficient. For the flight DSSCU, a dc to dc converter was secured from Power Cube Corporation that provides an efficiency of about 55 percent. It was necessary to make slight modification to meet the input current surge as specified in the ICD. The test results of the delivered dc to dc converter is shown in Table 3.

Power Flow

The DSSCU receives 22-34 V power from the spacecraft and transmits the same power to the QCM package. The power to each of the detectors is illustrated by the block diagram (Fig. 43). The power consumed by the QCM electronics depends upon the ambient temperature outside the QCM crystals. Switching is provided for turning off each of the detectors. Power will always be provided to the mux and uplink, no matter which detector is off.

Multiplexer

Since the multiplexer (mux) was a single link for data from all detectors it was decided to provide two multiplexers to improve the reliability. On command either mux A or B can be selected. A simple block diagram is illustrated in Fig. 44.

Environmental Tests

The DSS has passed the following environmental tests: Random Vibration, Thermal Cycling, Thermal Vaccum, Electromagnetic Interference (EMI), Electromagnetic Compatibility (EMC) and a Compatibility Test with the Ion Thruster Subsystem. The telemetry data was checked before and after each of these tests.

Random Vibration

The DSS electronics and detectors were mounted to a rigid fixture and vibrated in three mutually perpendicular axes at 20 GRMS (Fig. 45). The DSSCU enclosure was also vibrated at sine levels up to 9G (Fig. 46). One QCM and the warm solar cell located on the long boom was vibrated at 31.4 GRMS. Two ion collectors located on the lower boom were vibrated at 33.7 GRMS. The random vibration qualification level is considered to be at least 3 dB above the anticipated flight level.

Thermal Cycling

The DSSCU was subjected to nine cycles. One cycle was performed at temperature extremes of -30° to +60° C operating. The other flight cycles were performed at -50° and +80° C nonoperating. The soak time was a minimum of 4 hours.

Thermal Vacuum

The thermal vacuum was in an environment which simulates the maximum predicted on orbit thermal environment. The thermal vacuum was performed at a minimum pressure of $1x10^{-5}$ Torr using a chamber having a radiation shroud. The shroud remained cold during the testing. The DSSCU was exposed to three thermal cycles. The base plate which the DSSCU is attached is heated or cooled to obtain the extreme base plate temperatures. During the first or last cycle, the DSSCU is subjected to the extreme temperatures of -50° and +80° C nonoperating. The DSSCU is operated at +60° and -30° C for the other two cycles (Fig. 47).

Electromagnetic Interference (EMI) and Electromagnetic Compatibility (EMC)

The DSSCU was subjected to the EMI/EMC as defined by the ICD with Rockwell International. This included conducted emission of the power leads from 20 Hz to 50 M Hz, conducted susceptibility of power leads from 30 Hz to 400 M Hz and radiated emission and susceptibility of electric fields 14 K Hz to 18 G Hz.

Summary

The DSS is composed of two QCM's, nine solar cells, one potential probe and seven ion collectors. This set of hardware is considered adequate to measure the thruster efflux, material deposition and S/C potential relative to the local plasma in the vicinity of two 8-cm mercury ion thrusters. The flight data in conjunction with ground derived data will show that ion thrusters can be included in operational S/C.

The detectors and electronic units have passed all functional and environmental tests as specified. The analysis of the ground based data also indicate that the hardware is qualified for flight.

TABLE 1. - QCM FREQUENCY DATA IN HERTZ

Serial number	Beat frequency controlled temperature 25$^{+0.68}_{-0.54}$ in vacuum -20 to +50° C	Solar irradiance transients 0-1 sun	Crystal set	
			Reference	Active
1	2392-2418	2380-2425	9,968,300	9,965,400
4	1808-1829	1733-1803	9,967,000	9,964,500

TABLE 2. - COLD SOLAR CELL AND RADIATOR-Z MODULE-

PREDICTED THERMAL PERFORMANCE

Right ascention angle-vernal equinox		270°	210°	180°
Orbital average illumination	Solar cell (percent)	37.2	36.9	27.5
	Radiator (percent)	8.8	27.7	30.4
Temperature based on average illumination		-55° C	-45° C	-52° C
Temperature variation during orbit (°C)		11°	17°	16°
Final design with 1# added under radiator (variation)		5.5	8.5	8.0
Temperature-solar cell to solar cell (°C) differential		0.6	0.6	0.6
Temperature-solar cell to radiator (°C) differential		2	3	2
Temperature with 10 percent reflected solar load from spacecraft (°C) +3° C		-52		
Inclusion of heat load from ion engine at 150° C (°C) +7° C		-47		
Effect of mirrow degradation (add +3.2° C) °C α = -0.10		-44		
-X spacecraft surface module (+20°) (°C)		-24		

TABLE 3. - DC TO DC CONVERTER TESTS

	Voltage and current settings														
	210 V at 0.015 A			110 V at 0.040 A			18 V at 0.300 A			-18 V at 0.160 A			-40 V at 0.010 A		
Input volt.	22	28	34	22	28	34	22	28	34	22	28	34	22	28	34
Voltage output reading	211.1	211.0	211.4	110.2	110.2	110.7	18.1	18.1	18.07	-18.0	-18.0	-18.0	-40.2	-40.2	-40.3
Ripple volt. (PP)[a]	0.150	0.150	0.050	0.100	0.100	0.082	0.070	0.070	0.065	0.075	0.075	0.055	0.030	0.030	0.040
Voltage output limit	207.8 to 212.1	207.9 to 212.1	207.9 to 212.1	108.9 to 111.1	108.9 to 111.1	108.9 to 111.1	17.82 to 18.18	17.82 to 18.18	17.82 to 18.18	-17.82 to -18.18	-17.82 to -18.18	-17.82 to -18.18	-39.4 to -40.6	-39.4 to -40.6	-39.4 to -40.6
Line and load regulation VDC limit max./read.	3.15/0.049			1.65/0.052			0.27/0			0.27/0			0.60/0.007		

[a]Basic ripple only (10-60 kH3) 0.5 volt limit reflected ripple not to exceed 100 mV (reading max. = 80 mV).

TABLE 4. - DIAGNOSTIC SUBSYSTEM TELEMETRY OUTPUT

SEQUENCE SIGNAL LIST

Output order	Signal name	Comments
1	No Operation - Zeros	
2	Command Word	Data Bits C8 to C15
3	Potential Sensor Voltage	
4	Potential Sensor Current	
5	-40 Volt Attenuator	
6	+205 Volt Attenuator	
7	Ion Collector 4 Range	3 Bit Data
8	Ion Collector 4 Current	
9	Ion Collector 4 Voltage	
10	-18 Volt Attenuator	
11	+110 Volt Attenuator	
12	Ion Collector 1 Range	3 Bit Data
13	Ion Collector 1 Current	
14	Ion Collector 1 Voltage	
15	Bus Verify	6 Bit Data
16	Zero Calibration	
17	Ion Collector 2 Range	3 Bit Data
18	Ion Collector 2 Current	
19	Ion Collector 2 Voltage	
20	+18 Volt Attenuator	
21	DSSCU Temperature	
22	Ion Collector 3 Range	3 Bit Data
23	Ion Collector 3 Current	
24	Ion Collector 3 Voltage	
25	Clock Selected	2 Bit Data
26	Full Scale Calibration	
27	Ion Collector 5 Range	3 Bit Data
28	Ion Collector 5 Current	
29	Ion Collector 5 Voltage	
30	Solar Cell C1 Warm Temperature	
31	Solar Cell C1 Detector Output	
32	Ion Collector 6 Range	3 Bit Data
33	Ion Collector 6 Current	
34	Ion Collector 6 Voltage	
35	Solar Cell C7 Cold Temperature	
36	Solar Cell C7 Detector Output	
37	Ion Collector 7 Range	3 Bit Data
38	Ion Collector 7 Current	
39	Ion Collector 7 Voltage	
40	Radiator R7 Temperature	
41	TQCM Beat Frequency 1	Data Bits 2^8 to 2^{15}
42	TQCM Beat Frequency 1	Data Bits 2^0 to 2^7
43	Potential Sensor Voltage	
44	TQCM Temperature Sensor 1	
45	Radiator R5 Temperature	
46	Solar Cell C8 Warm Temperature	
47	Solar Cell C5 Cold Temperature	
48	Solar Cell C5 Detector Output	
49	Solar Cell C8 Detector Output	
50	Radiator R9 Temperature	
51	Solar Cell C2 Cold Temperature	
52	Solar Cell C9 Cold Temperature	
53	Solar Cell C9 Detector Output	
54	Solar Cell C2 Detector Output	
55	Radiator R2 Temperature	
56	TQCM Beat Frequency 2 MSB	Data Bits 2^8 to 2^{15}
57	TQCM Beat Frequency 2 LSB	Data Bits 2^0 to 2^7
58	TQCM Temperature Sensor 2	
59	Solar Cell C6 Detector Output	
60	Solar Cell C6 Warm Temperature	
61	Solar Cell C3 Warm Temperature	
62	Solar Cell C4 Warm Temperature	
63	Solar Cell C4 Detector Output	
64	Solar Cell C3 Detector Output	

All measurements are 200 milliseconds apart.

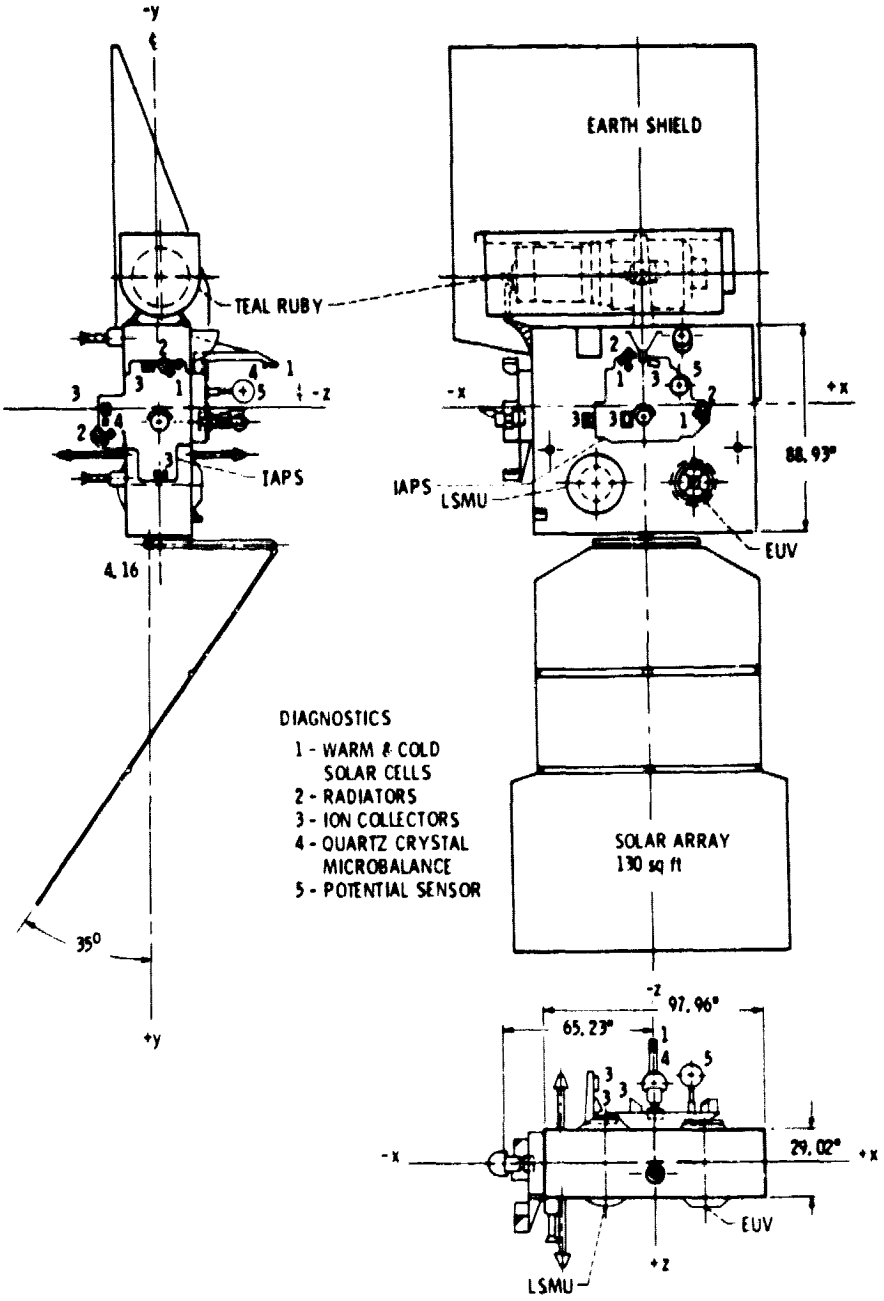

Figure 1. - IAPS & P80-1 experiments.

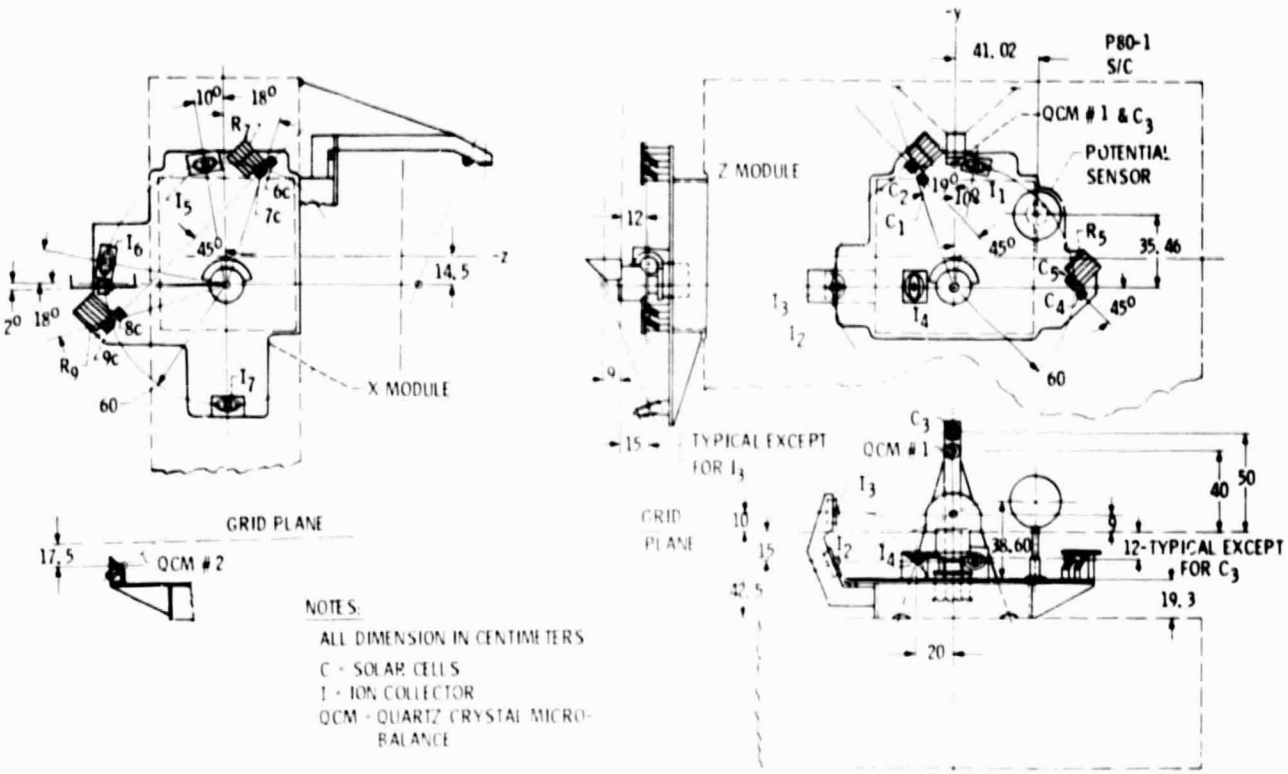

Figure 2. - Diagnostics - location.

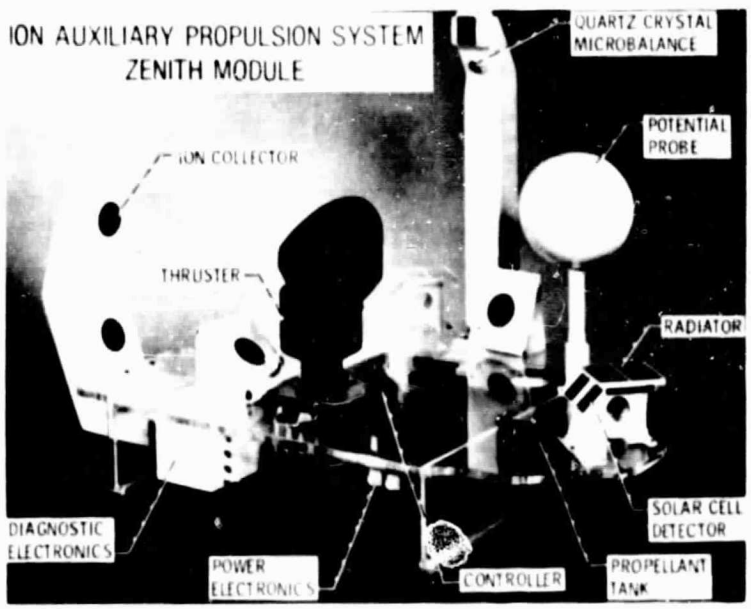

Figure 3. - Ion auxiliary propulsion system zenith module.

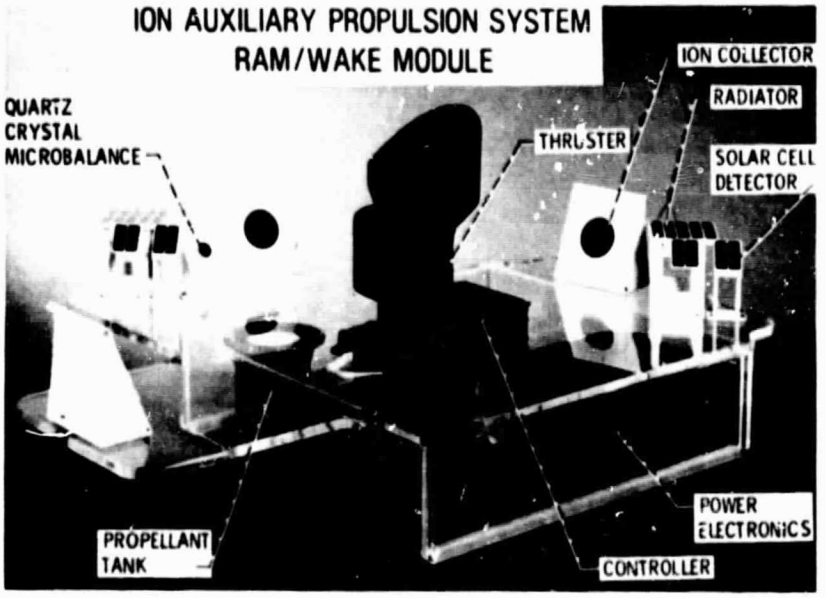

Figure 4. - Ion auxiliary propulsion system ram/wake module.

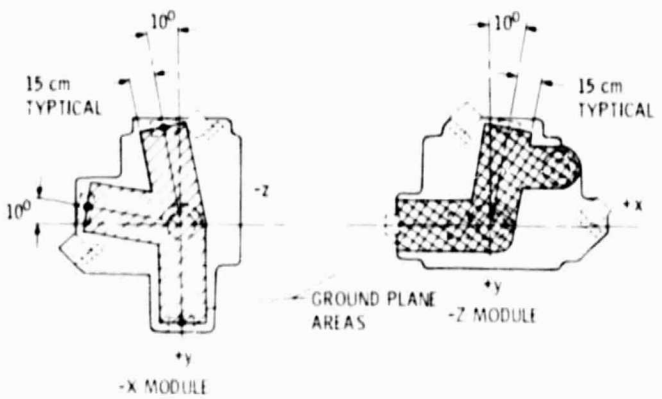

Figure 5. - Diagnostic - ground plane requirements on modules.

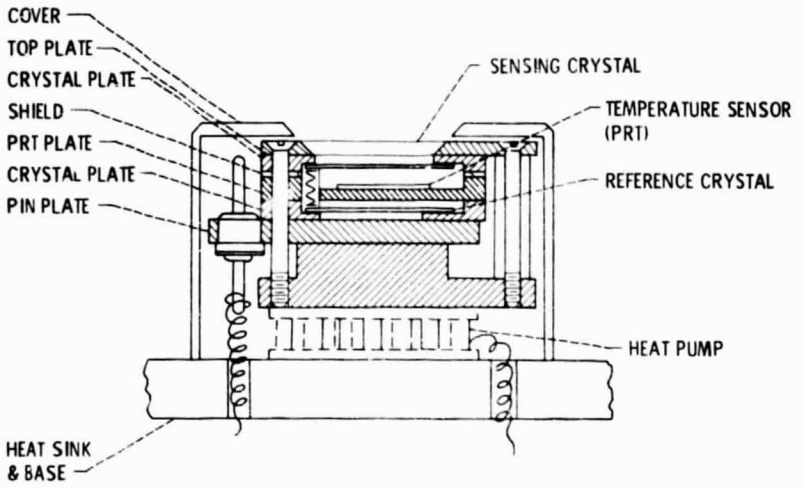

Figure 6. - QCM Head assembly.

Figure 7. - QCM Detector

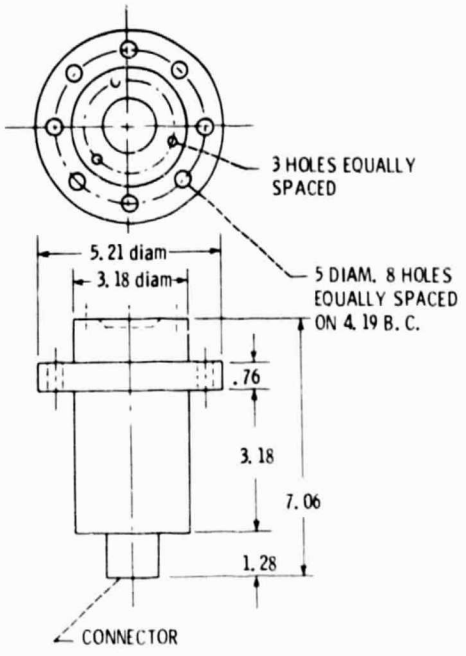

Figure 8. - QCM Detector. Full scale - all dimensions in centimeters; weight = 350 grams.

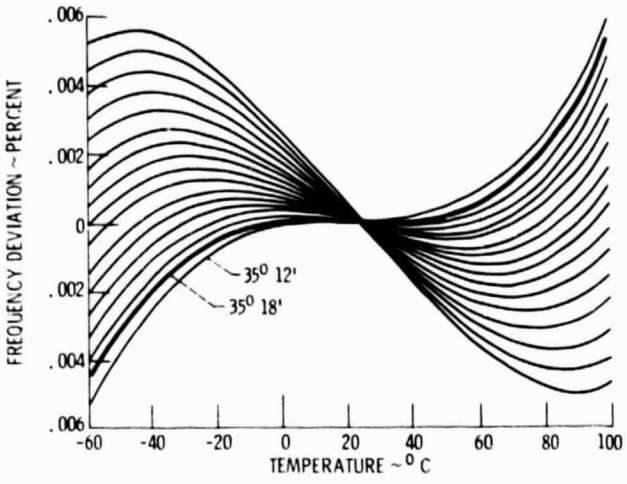

Figure 9. - Frequency vs temperature for different zero - coefficient temperatures.

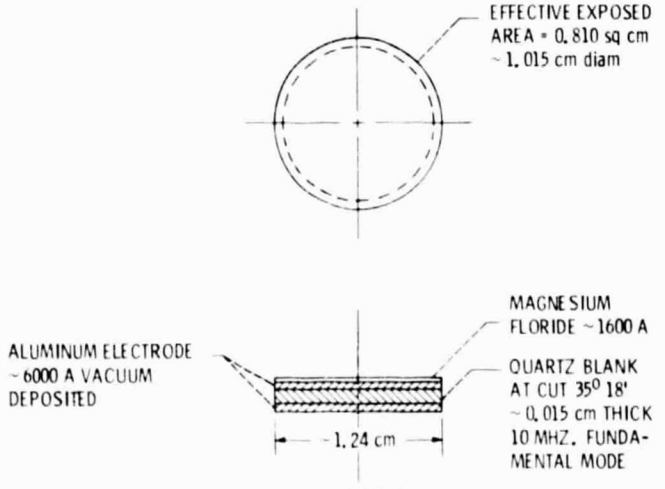

Figure 10. - Detector crystal design (no scale).

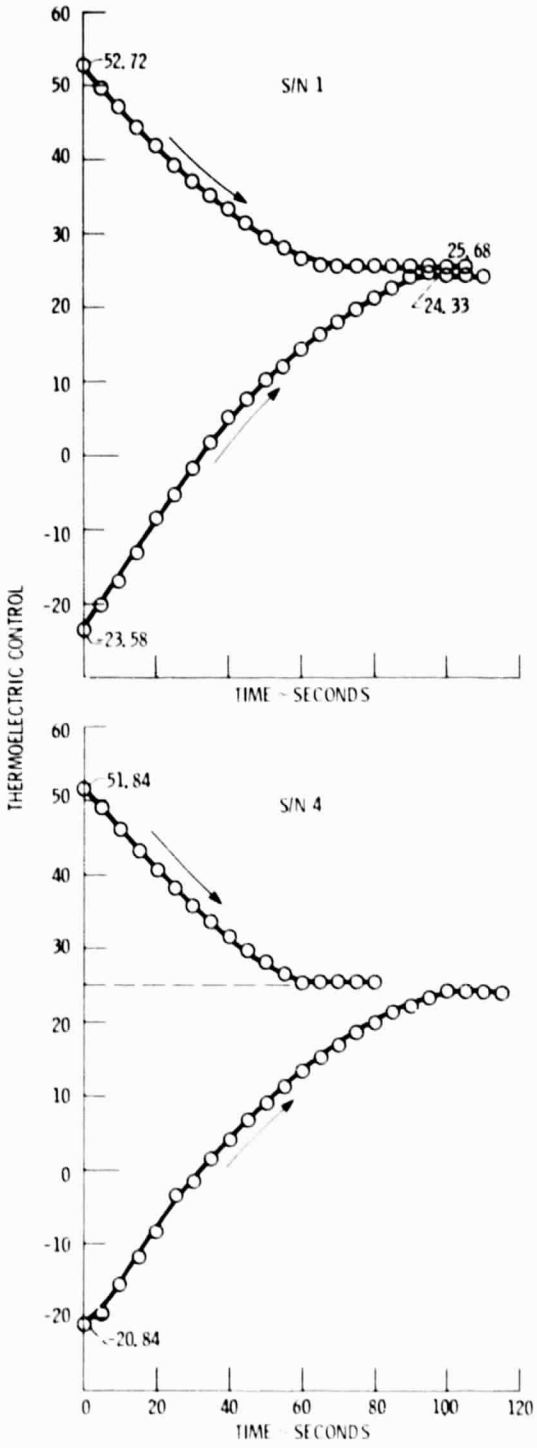

Figure 11. - Thermoelectric control - time vs temperature (hot & cold to normal operation).

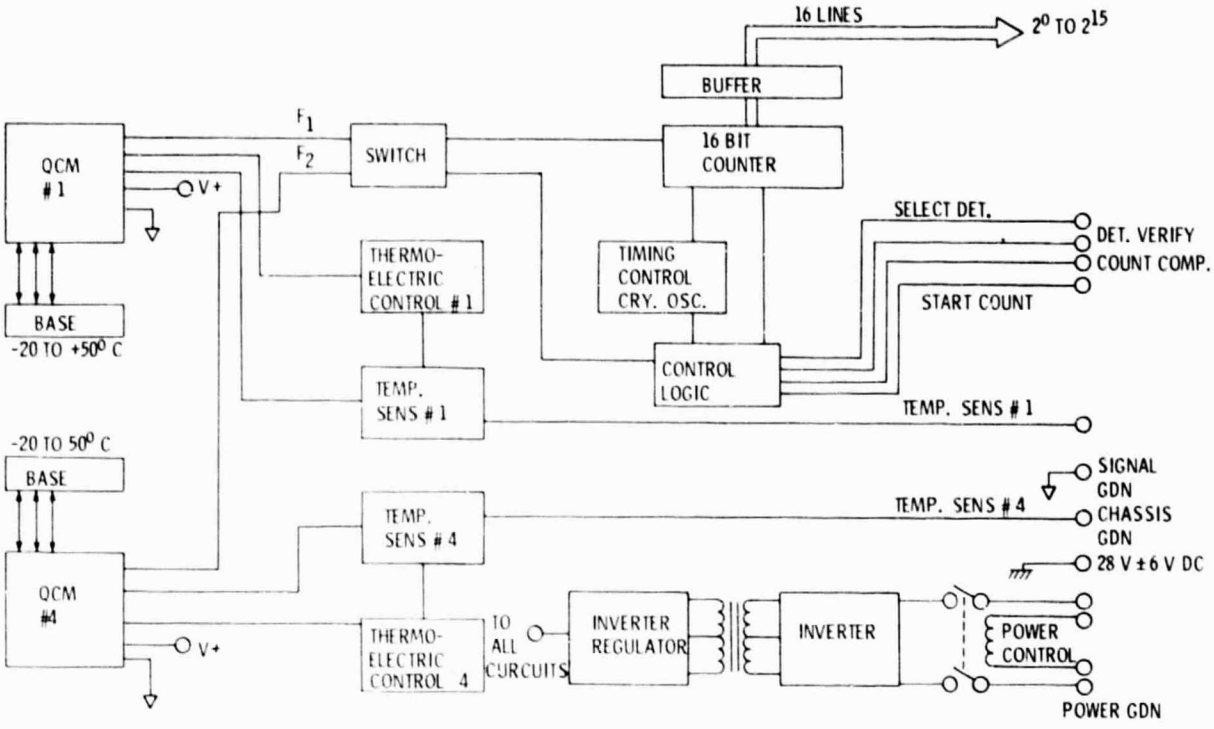

Figure 12. - QCM - electrical block diagram.

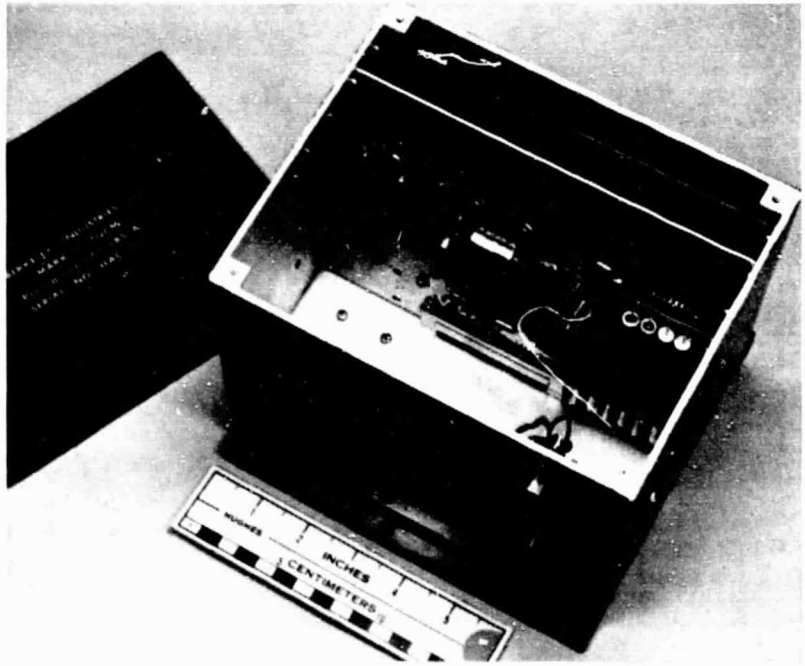

Figure 13. - QCM electronics.

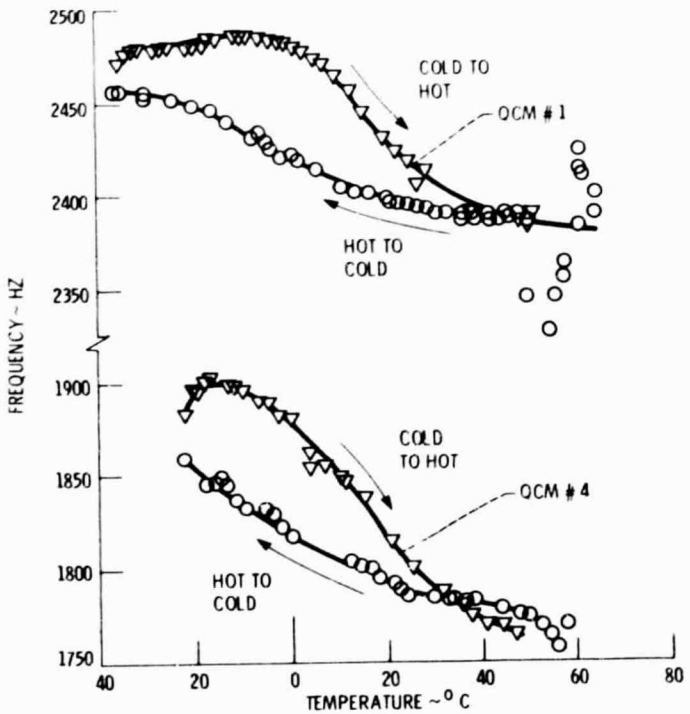

Figure 14. - QCM - serial#1 & 4 (MK 10) without thermal control. QCM temperature vs frequency.

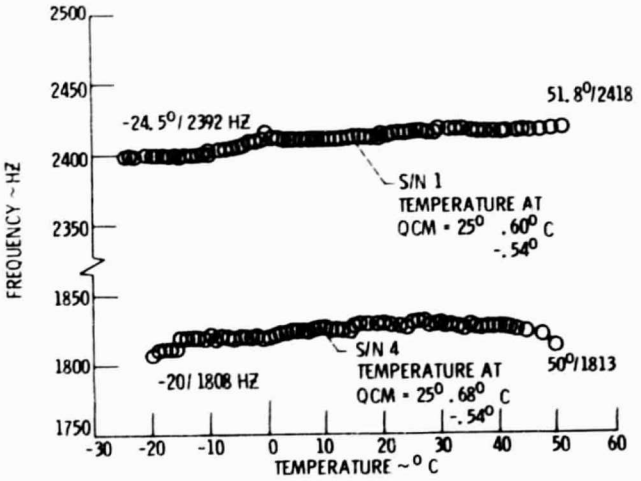

Figure 15. - QCM serial number 1 & 4 (MK 10) with thermal control. Base plate temperature vs frequency.

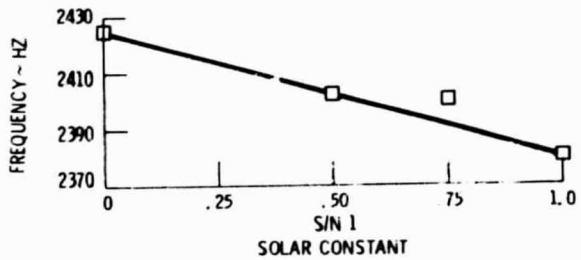

Figure 16. - Solar irradiance induced transients.

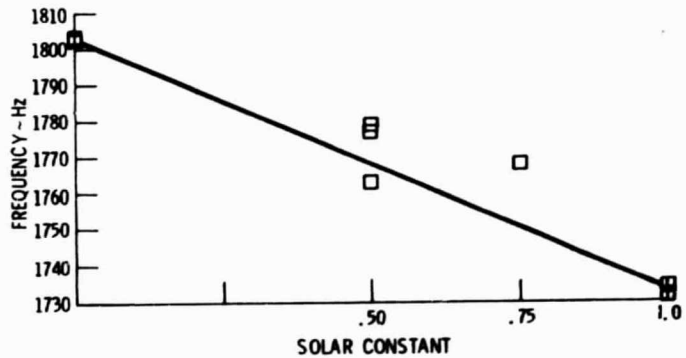

Figure 17. - Solar irradiance induced transients.

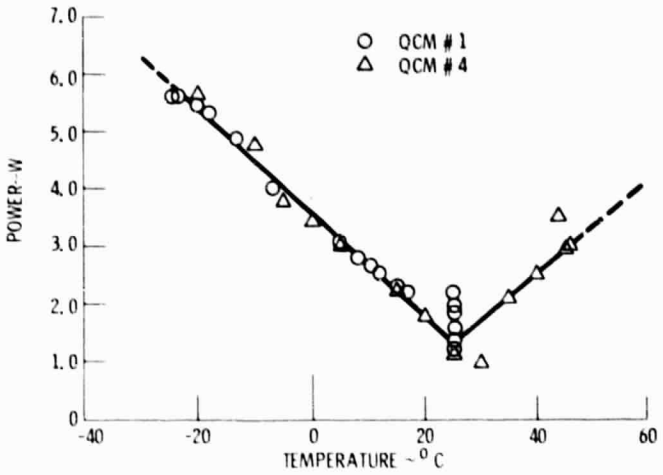

Figure 18. - Power required to operate QCM # 1 & 4 from -20° to 50° C.

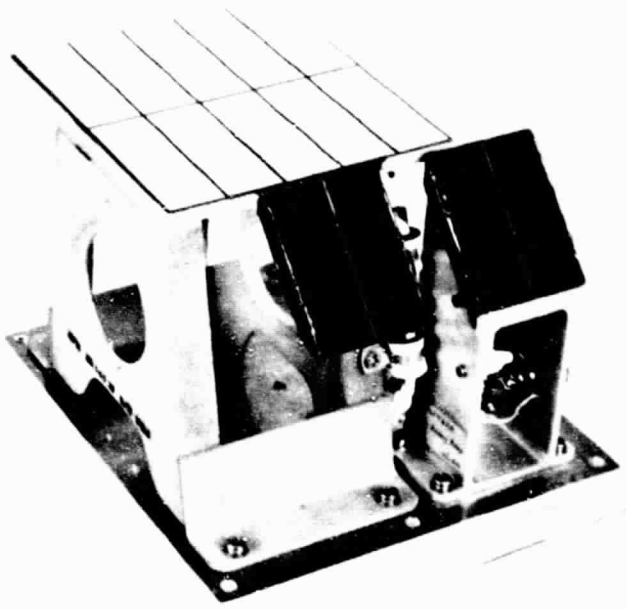

Figure 19. - Cold solar cell, radiator & warm solar cell array.

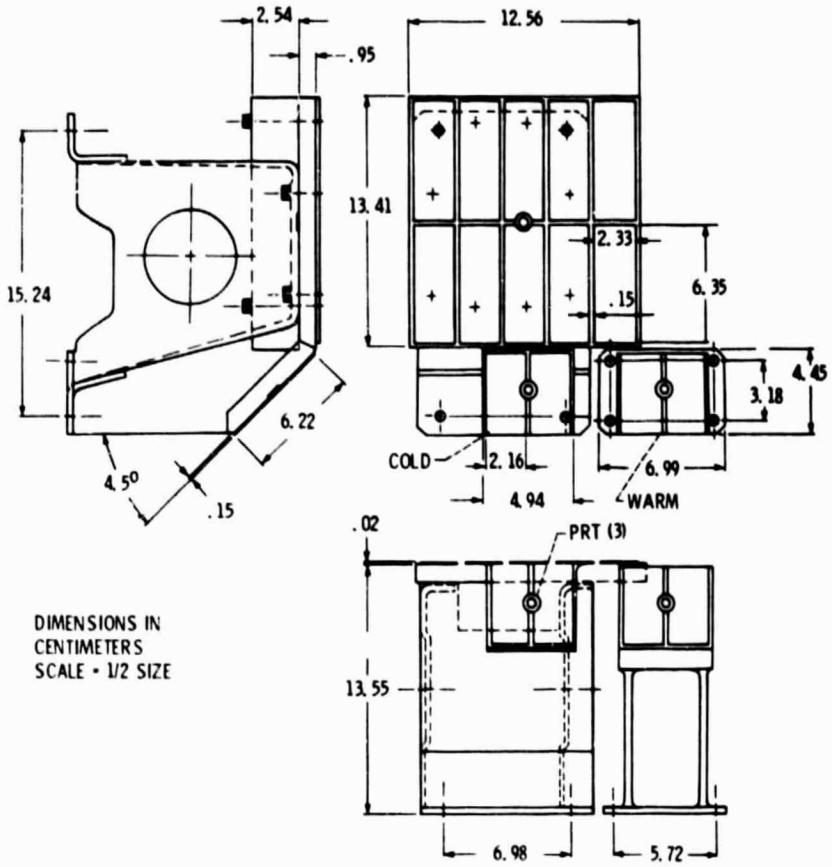

Figure 20. - Solar cell & radiator mounting & arrangement.

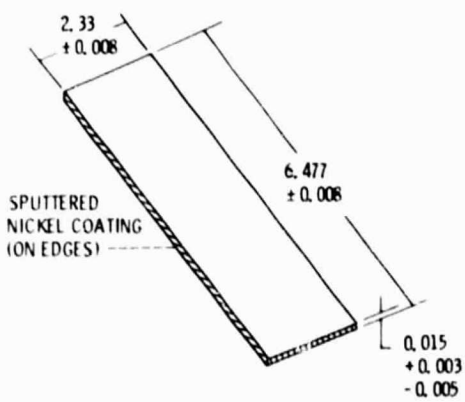

FUSED SILICA CORNING CODE 7940

SOLAR ABSORTANCE
α TOTAL NORMAL $\leq$ 0.07

REFLECTIVE SILVER COATING, WITH OVERCOAT LAYERS OF INCONEL & INDIUM OXIDE

SOLAR ABSORPTANCE MEASURED OVER A WAVELENGTH OF 0.3 TO 2.12 MICRONS

RTV-566 MIXED WITH 10% CARBON USED AS ADHESIVE FOR ATTACHING MIRRORS TO RADIATOR - GROUNDING STATIC CHARGE

NICKEL COATING FOR CONDUCTING STATIC CHARGE TO ADHESIVE

Figure 21. - Cover glass (mirror).

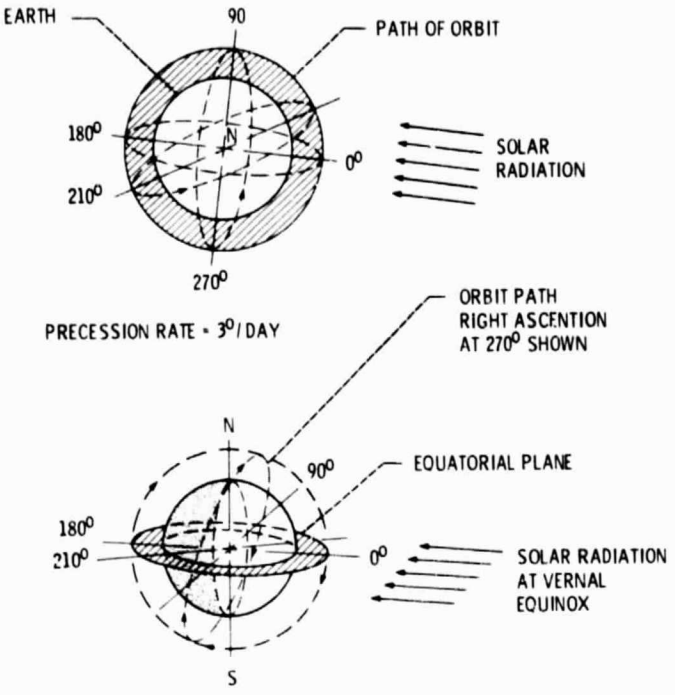

Figure 22. - Orbital paths for thermal analysis program - zenith module.

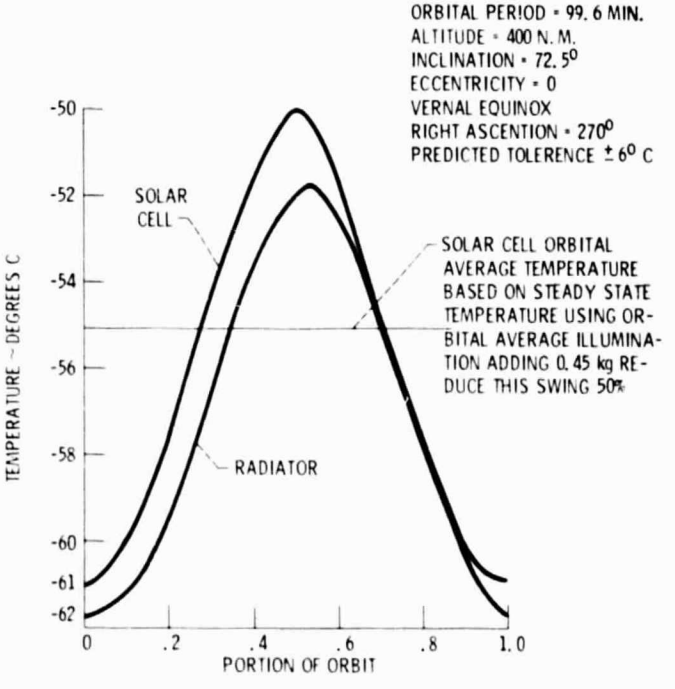

Figure 23. - Cold solar celleradiator - 2 orbital variation with temperature.

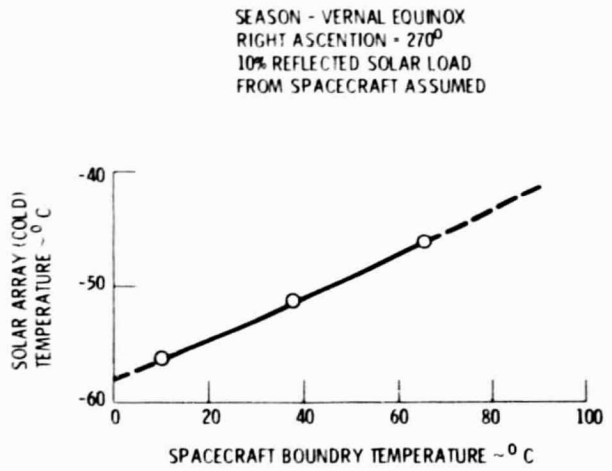

Figure 24. - Cold solar array temperature vs spacecraft boundary temperature.

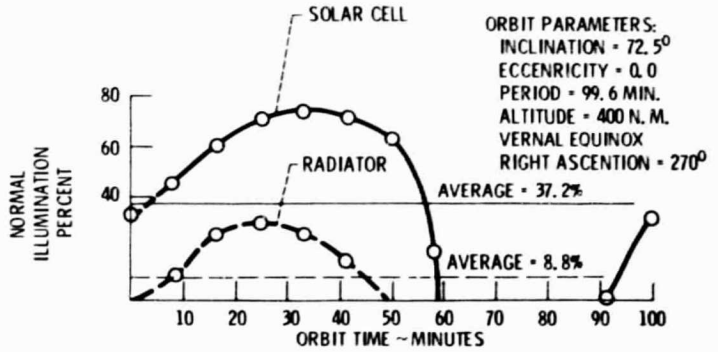

Figure 25. - Solar cell & radiator - z module normal solar illumination vs time in percent.

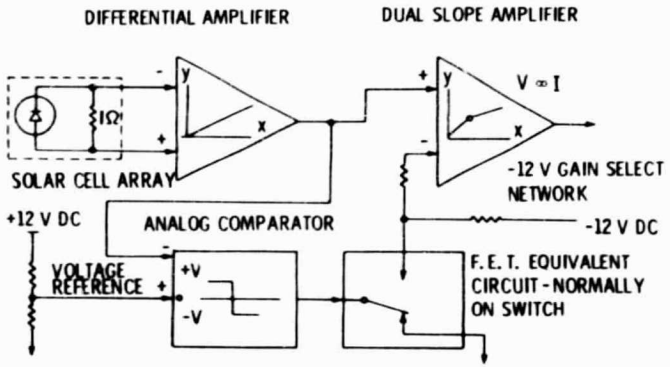

Figure 26. - Solar cell electronics - block diagram.

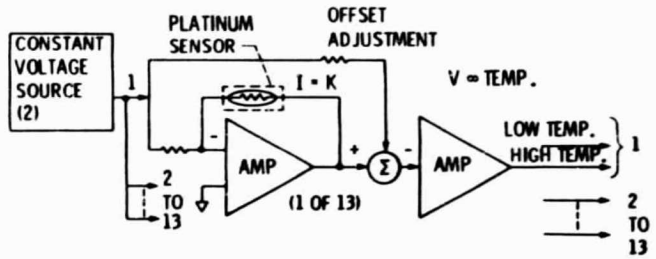

Figure 27. - Temperature sensor electronics functional block diagram.

$$\frac{2.5}{.04} = -62.5$$

$-62.5 - 40 = -102.5$

$$\frac{5.12}{.04} = 128$$

$128 - 102.5 = 25.5$

$$\frac{2.5}{.04} = 62.5$$

$-62.5 + 35 = -27.5$

$$\frac{5.12}{.04} = 128$$

$128 - 27.5 = 100.5$

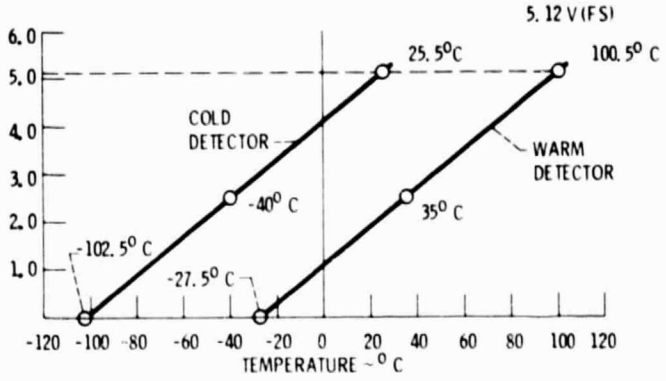

Figure 28. - Temperature sensors - dual range. Solar cell detector - characteristic curves.

	25° C	-100° C	100° C
SHORT CIRCUIT CURRENT	549.4 mA	495.1 mA	598.8 mA
RADIATED 1×10^{14} E/CM^2	524.7	452.3	580.8
OPEN CIRCUIT VOLTAGE	592.5 mV	873.6 mV	422.2 mV
RADIATED 1×10^{14} E/CM^2	562.3	821.2	413.8

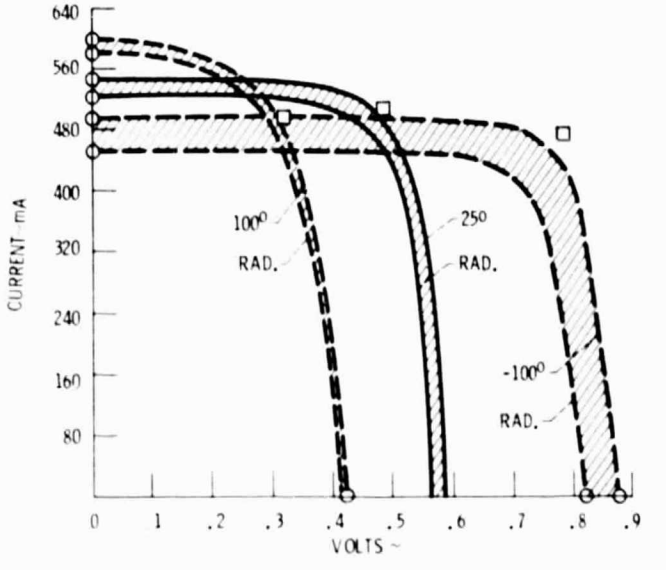

Figure 29. - Solar cell calibration curves. Non radiated & radiated (1×10^{14} electrons per square centimeter) for 25, -100 & 100° C.

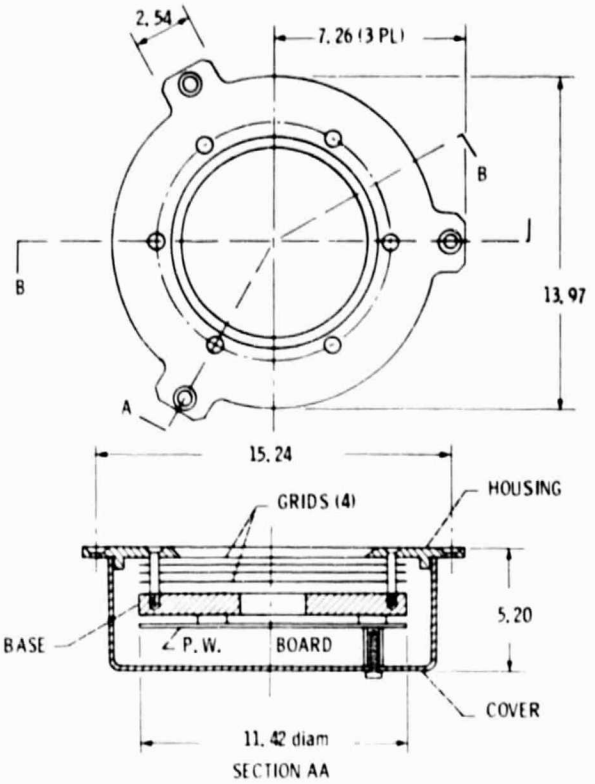

Figure 30. - Ion collector detector.

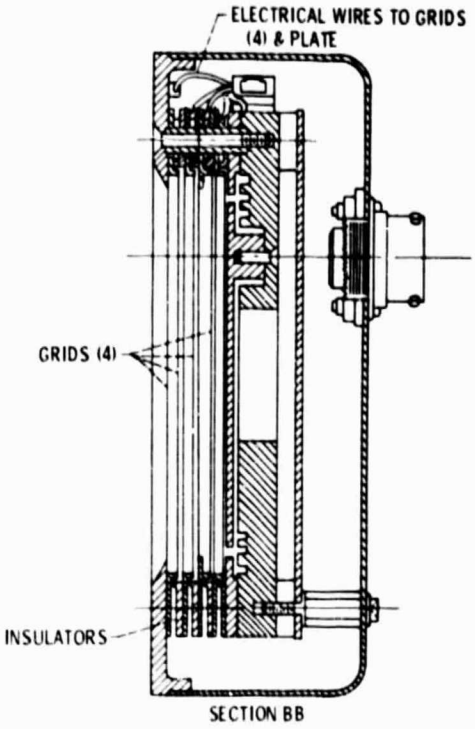

Figure 31. - Ion collector dector.

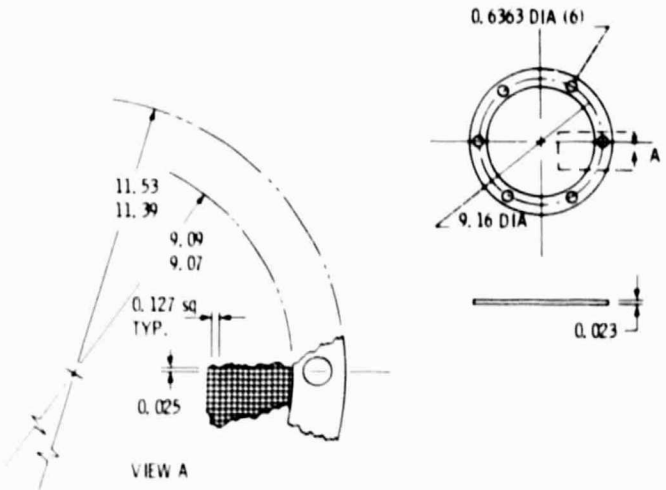

Figure 32. - Screen grid.

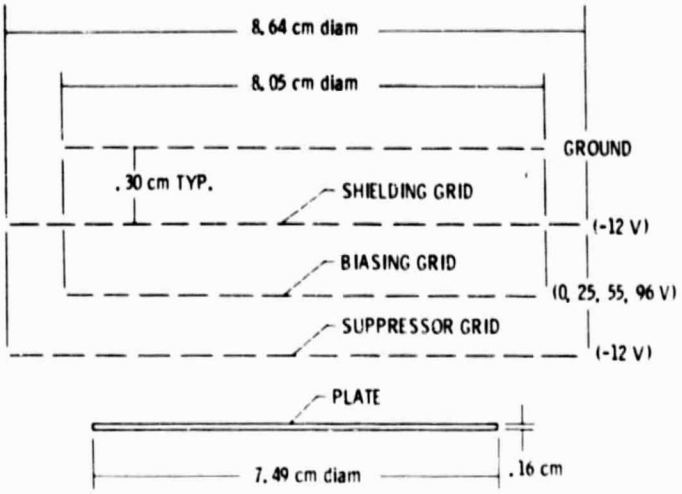

Figure 33. - ion collector grid & plate size, spacing & potential.

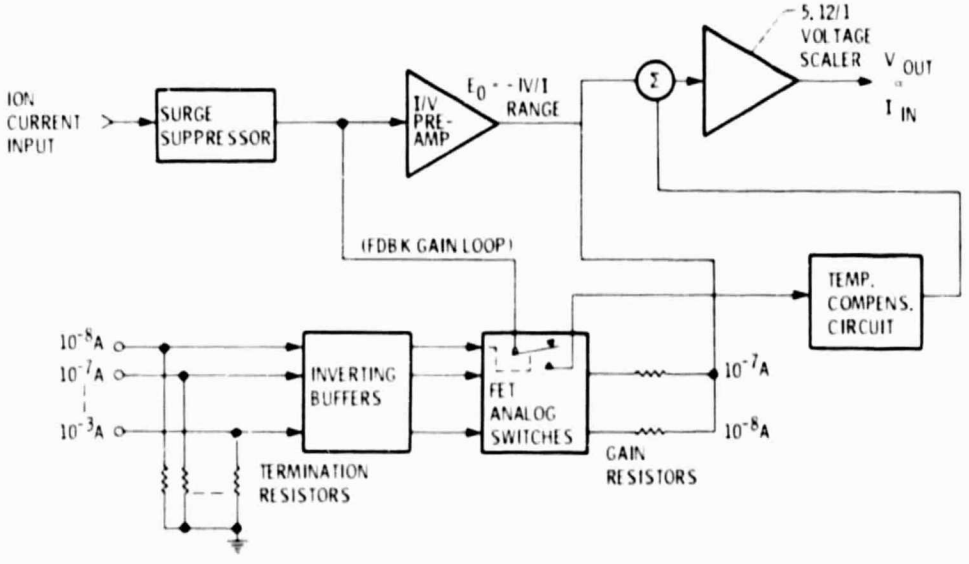

Figure 34. - Pre - amplifier/scaler block diagram.

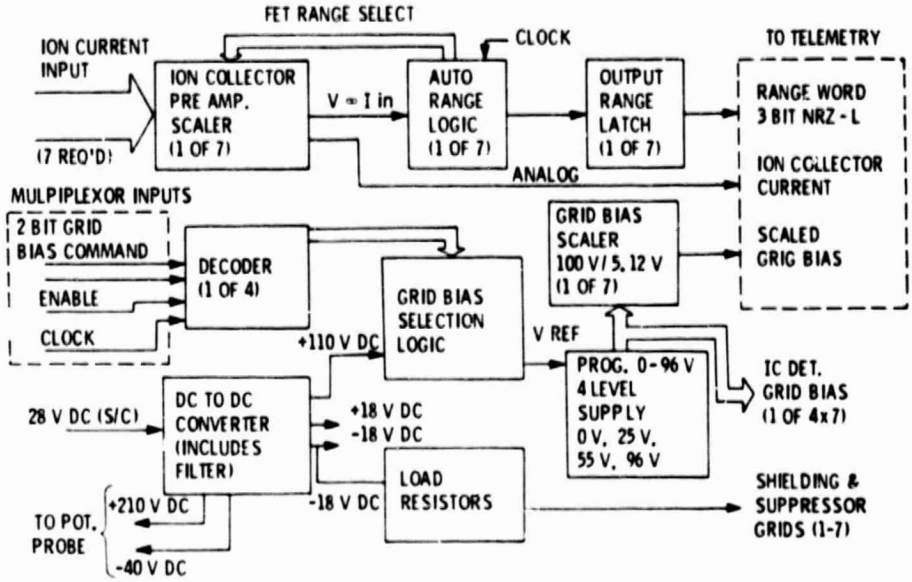

Figure 35. - Ion collector electronics - system block diagram.

Figure 36. - Potential probe (detector).

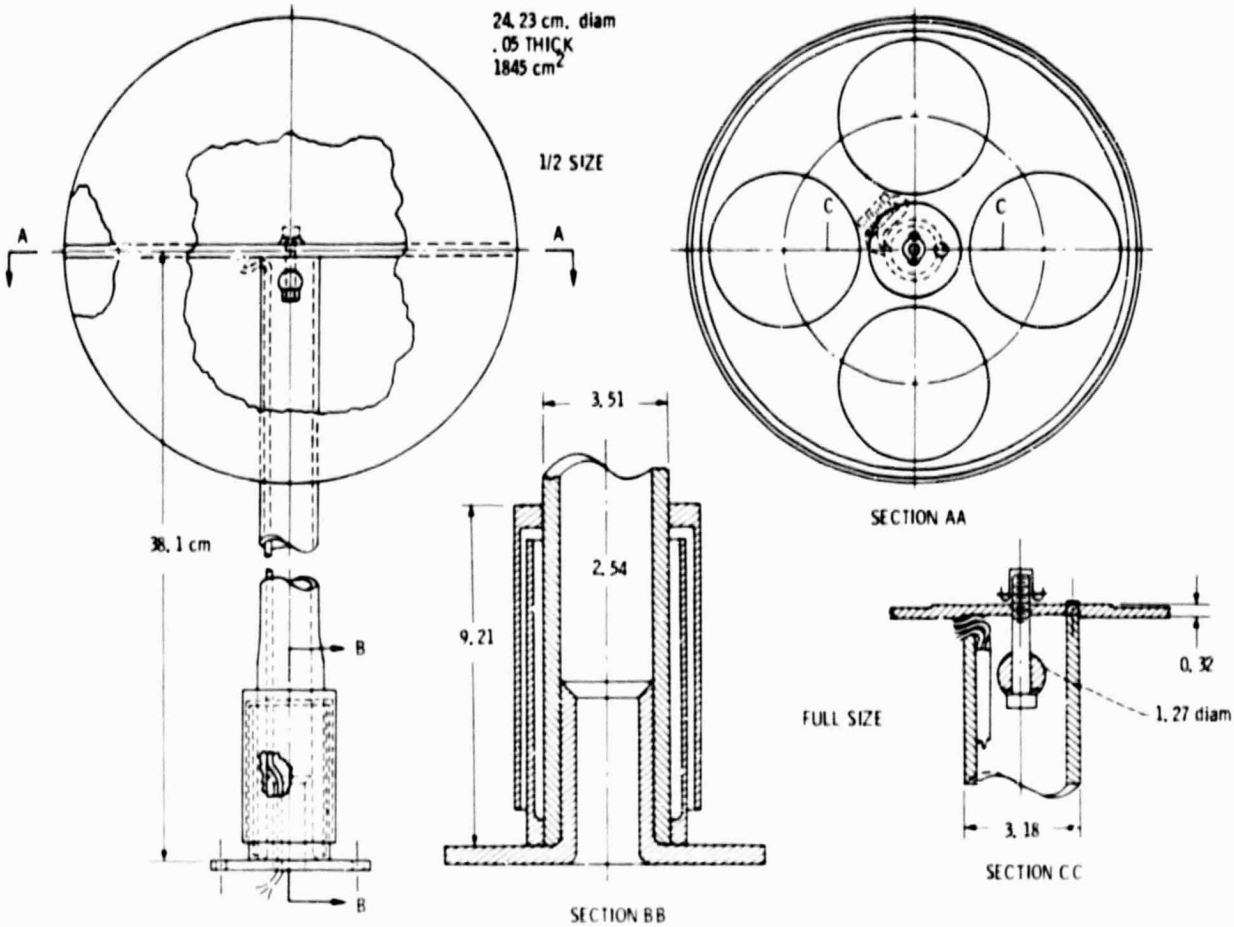

Figure 37. - Potential probe.

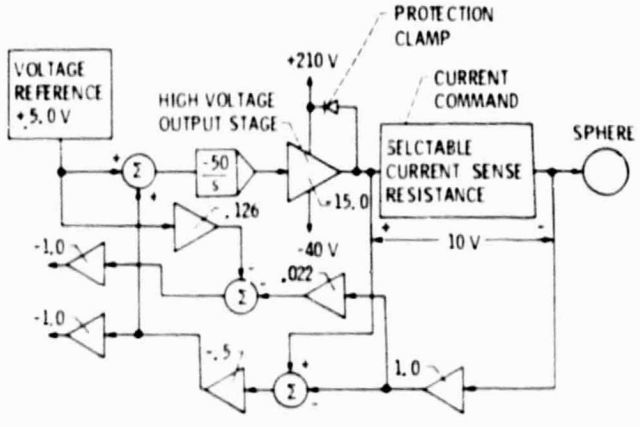

NOTE:

TELEMETRY "BIAS VOLTAGE" IS 0 VOLTS AT SPHERE BIAS VOLTAGE OF -25.0 V. SLOPE IS IV/40 V. TELEMETRY "SPHERE CURRENT" IS 0 VOLTS AT NULL CURRENT SLOPE IS 20% FS/V.

Figure 38. - Spacecraft potential probe block diagram.

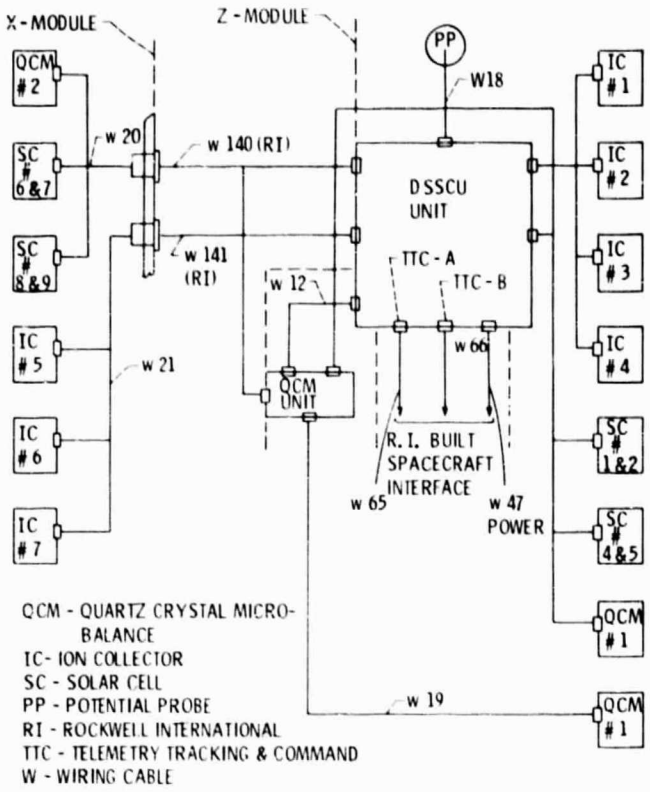

Figure 39. - Diagnostic subsystem functional block diagram.

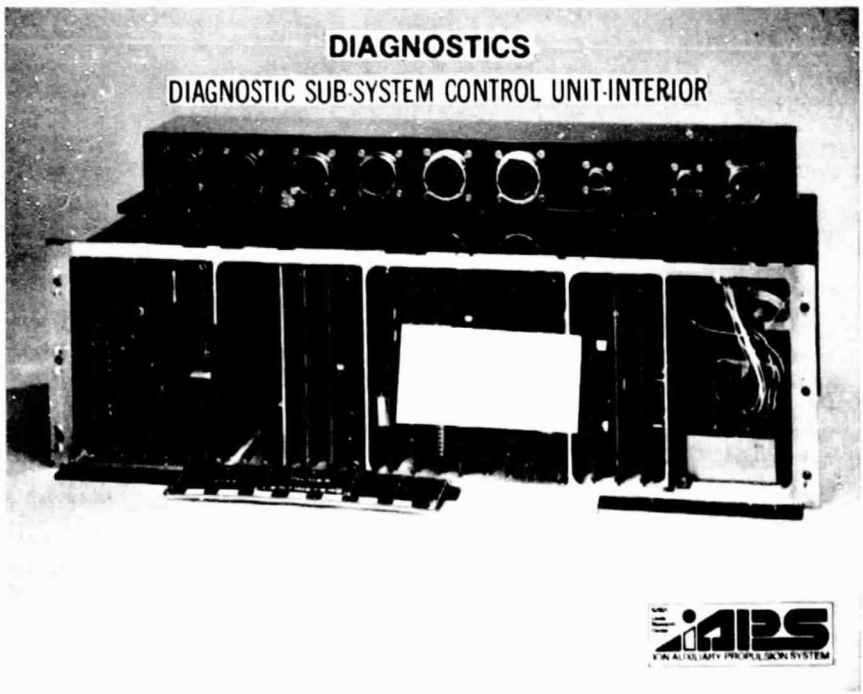

Figure 40. - Diagnostics.

1-7 - AUTO LOGIC GRID BIAS
8 - GRID BIAS SELECTION
9 - TEMPERATURE SENSORS
10 - SOLAR CELLS
11 - UPLINK
12 - MULTIPLEXER A - I
13 - MULTIPLEXER A - II
14 - MULTIPLEXER A - III
15 - MULTIPLEXER B - I
16 - MULTIPLEXER B - II
17 - MULTIPLEXER B - III
18 - POTENTIAL PROBE - I
19 - POTENTIAL PROBE - II
20 - POWER DISTRIBUTION

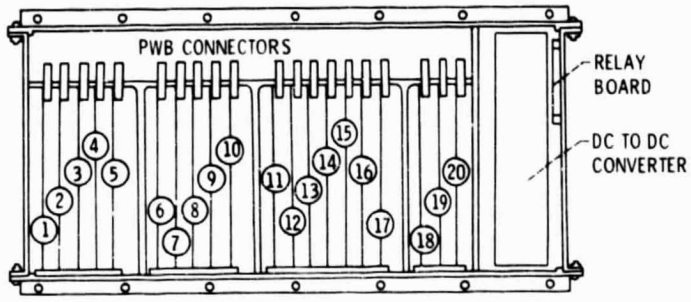

Figure 41. - DSSCU electronics.

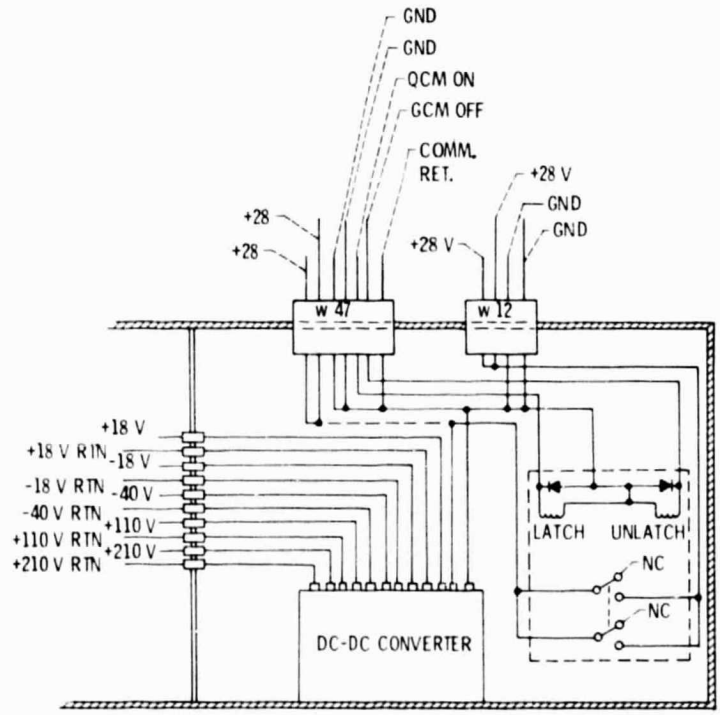

Figure 42. - DC to DC converter.

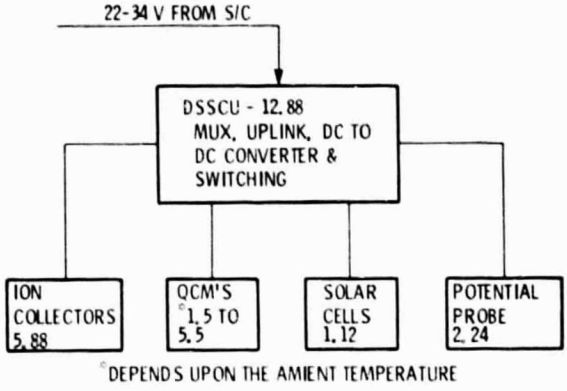

Figure 43. - Power flow in watts.

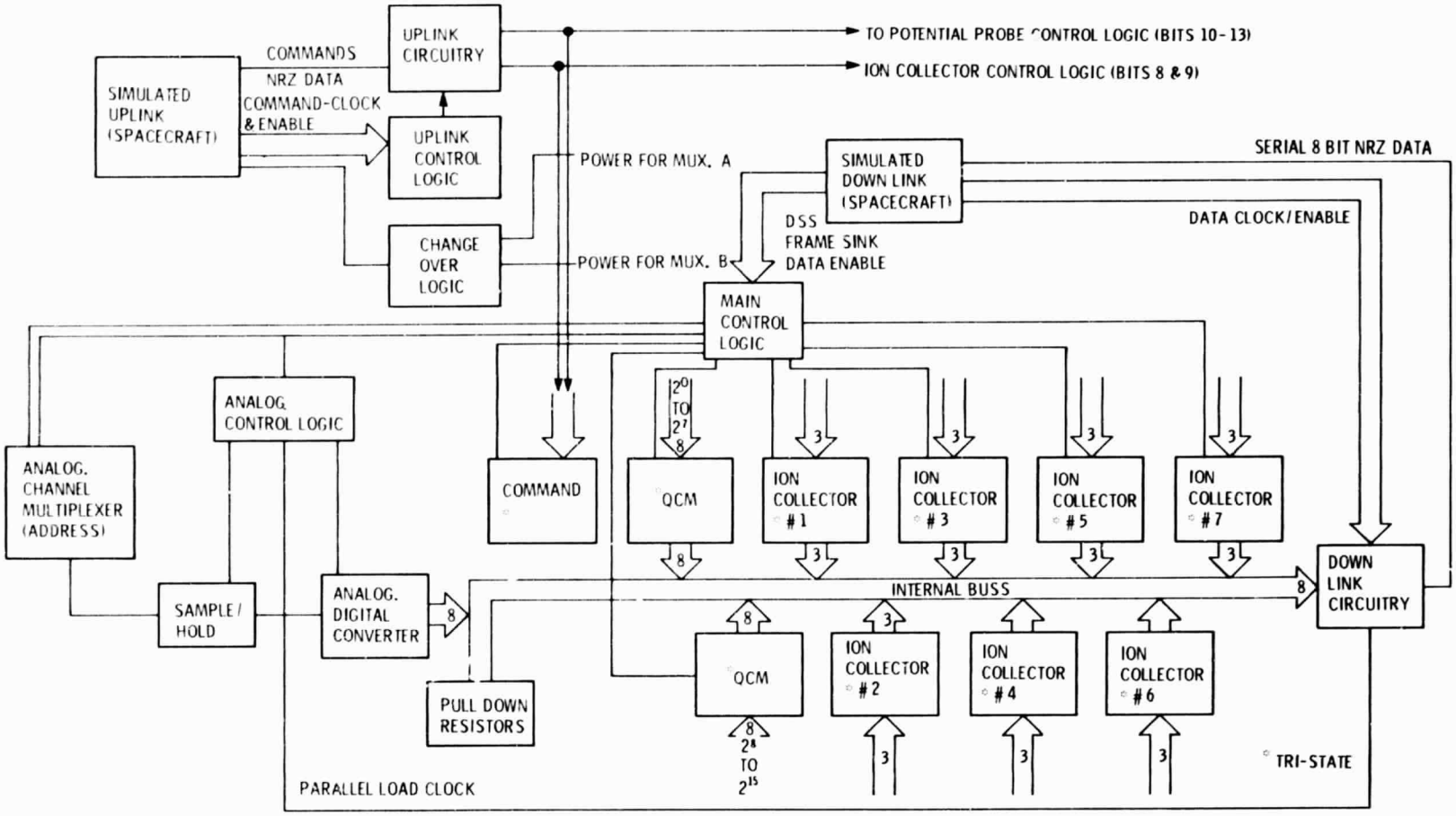

Figure 44. - Multiplexer block diagram.

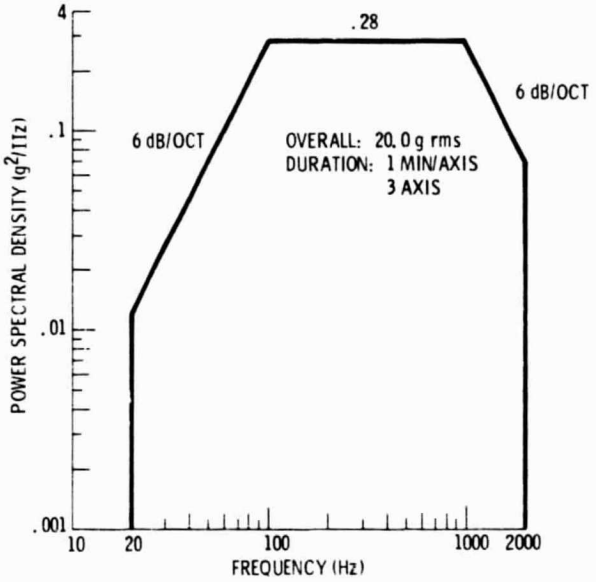

Figure 45. - Random vibration.

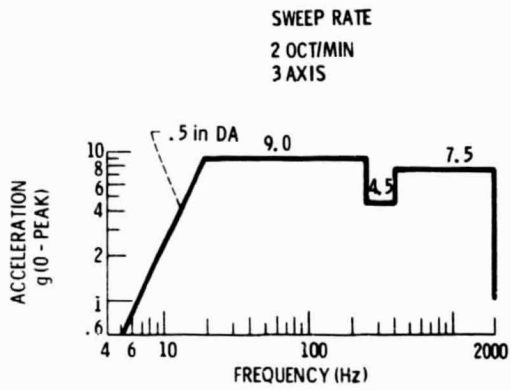

Figure 46. - Sinusoidal vibration (environmental verification level).

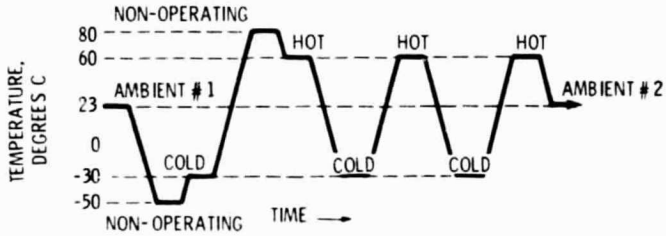

NOTES:

(1) MAINTAIN TEMPERATURE LEVELS FOR AT LEAST 4 HOURS BEFORE OPERATING DSSCU.

(2) THE DSSCU SHALL OPERATE ONLY WHEN THE TEMPERATURE IS WITHIN THE LIMITS -30 to 60 DEGREES C.

(3) THE VACUUM SHALL BE LESS THAN 10^{-5} TORR.

Figure 47. - DSSCU thermal vacuum test cycle.